Chapter 5
Outcomes from Field Measurements on the Magerholm Ferry Quay: System Identification, Finite Element Model Updating and Sensitivity Analysis

Ba Tung Le, Bartosz Siedziako, Torodd Skjerve Nord, and Luigi Sibille

Abstract Structural health monitoring (SHM) has become an essential practice in the research community due to the necessity of maintaining the longevity and safety of critical infrastructure. The Magerholm ferry quay examined in this study is an example of coastal infrastructure exposed to harsh environmental conditions and complex operational loads. As an important part of the region's transportation network, the quay accommodates significant daily traffic, including both local commuters and commercial vehicles. Despite that, previous SHM research has mainly focused on traditional bridge structures, leaving a considerable gap in our understanding of the health and performance of these equally vital maritime structures. This study explores various aspects of structural health monitoring for a linkspan (ferry docking bridge) using field measurements, system identification, finite element model updating (FEMU), and sensitivity analysis of the Magerholm linkspan.

Keywords Structural Health Monitoring · Link-span · System Identification · Finite Element Model Updating · Sensitivity Analysis

Introduction

The development of human society is linked to infrastructure development. As more and more structures near or exceed their design life, monitoring and maintenance have become increasingly challenging and expensive [1–3]. This issue is exacerbated by the increasingly harsh weather conditions attributed to global warming, particularly accelerating the deterioration of coastal infrastructure. To address this, researchers have been developing innovative techniques for asset condition monitoring, maintenance optimization, and life prediction [4–7].

Ferry terminals and their supporting infrastructure, for example linkspans, are critical components of the economies of coastal and island nations like Norway. These structures are subjected to harsh marine conditions and the excessively repeated impact of docking ferries [8], leading to structural damages [9]. One such damage example is the reduction of support provided by the lifting tower (Fig. 1), a critical component of a linkspan that supports the docking platform vertically and houses the jack used to adjust the bridge's height to accommodate varying tidal levels. Excessive operation can compromise the structural integrity of these towers. Despite their significance, our understanding of the behavior of lifting towers remains limited. It is clear that there is a need for further research on linkspans, with a particular focus on the behavior and health of lifting towers.

This study investigates the dynamic behavior of Magerholm linkspan through a combination of field experiments, system identification, and finite element modeling. Firstly, FEMU is also applied to accurately determine the actual condition of the lifting tower through the stiffness of the springs representing it. Afterwards, a sensitivity analysis was conducted to evaluate the influence of lifting tower stiffness on the dynamic behavior of ferry docks, with the aim of determining whether such damage could be easily detected. The results demonstrate that the natural frequencies of ferry docks are highly sensitive to lifting tower stiffness, particularly the first bending and first torsion modes.

B. T. Le (✉) · Bartosz Siedziako · Torodd Skjerve Nord · Luigi Sibille
Department of Ocean Operations and Civil Engineering, Norwegian University of Science and Technology, Larsgårdsvegen 2, 6009 Ålesund, Norway
e-mail: batung.le@ntnu.no; bartosz.siedziako@ntnu.no; torodd.nord@ntnu.no; luigisi@ntnu.no

Brian Damiano et al. (eds.), *Structural Health Monitoring & Machine Learning, Vol. 12*, Conference Proceedings of the Society for Experimental Mechanics Series, https://doi.org/10.13052/97887-438-0157-3_5

Field measurement

Magerholm Ferry Dock

The Magerholm ferry quay is part of Route 60, which connects Magerholm and Sykkylven. This route plays a vital role in the transportation system of the Møre og Romsdal area, with an average daily traffic of up to 2,500 vehicles [10]. This structure is composed of two main components: the steel docking bridge or so called linkspan and the side support quay (concrete bridge), as illustrated in Figs. 1 and 2. The linkspan is 16m long, 7m wide and constructed of steel. The bridge deck consisting of main longitudinal beams connected by cross beams and diagonal braces for structural stabilization. Since the structure is used for ferry docking, it must accommodate varying tide heights by adjusting the height of the ferry quay to match the ferry. To achieve this, lifting towers are employed; they are connected to a lifting beam located beneath the deck, serving as the support for the docking bridge. The other support is provided by the abutment, which includes conical fenders

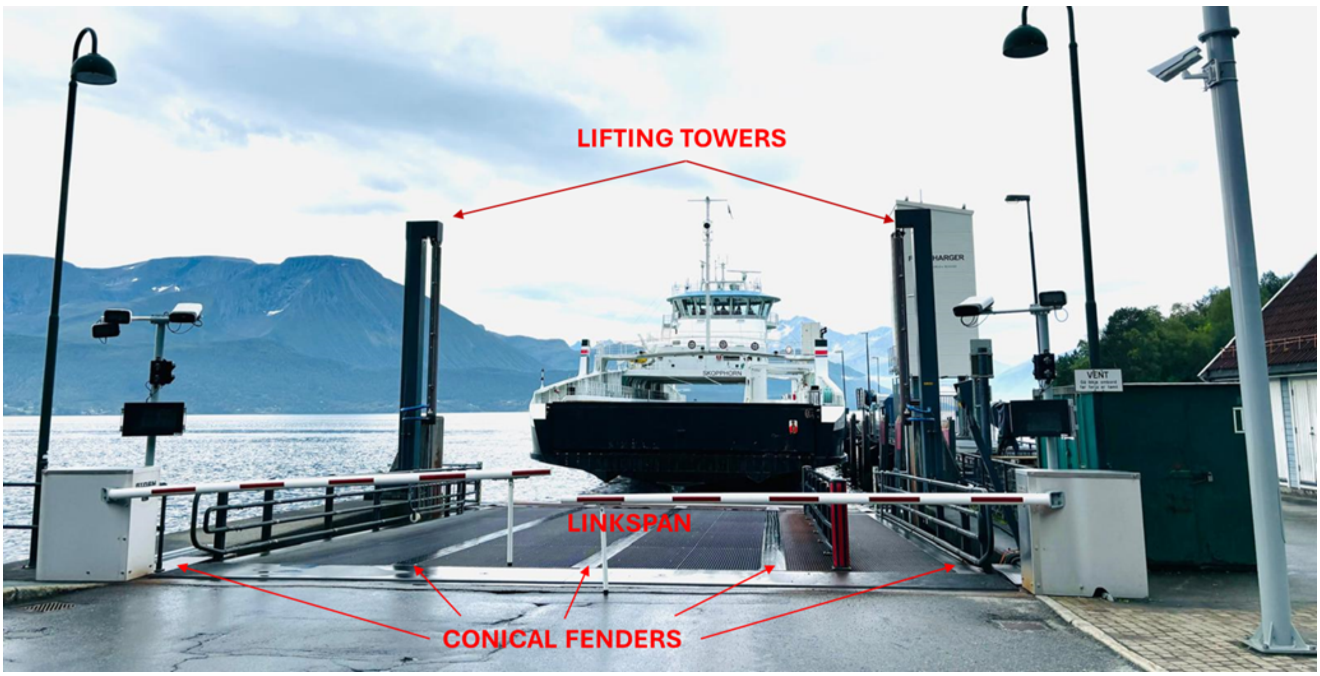

Fig. 1 Magerholm ferry quay with its structural components

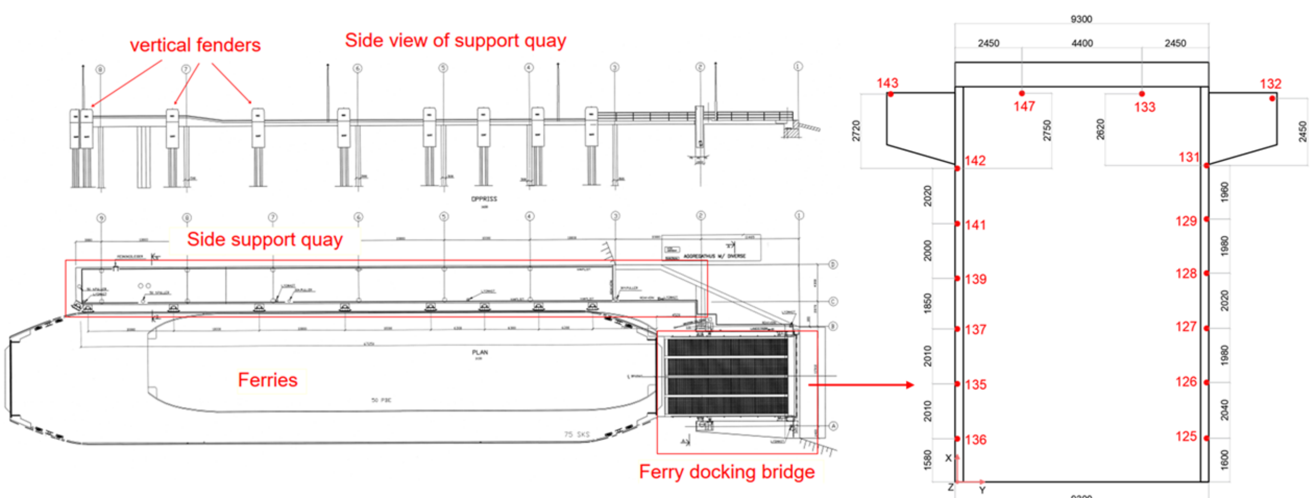

Fig. 2 Magerholm ferry dock sensor layout

beneath the main beam to absorb the impact from docking ferries. Above these components, steel grating are installed to accommodate movement of vehicles and passengers. It should be noticed that when the ferry is successfully docked, the lifting towers then release the jacks and the new support to the dock is the ferry itself. Field experiments presented in this studies were conducted in the ”free state” when ferry dock bridge was supported by the lifting towers.

Field Measurement Setup

The installation and measurement of sensors on the ferry dock were conducted on May 31, 2022. For this measurement, G-Link 200 wireless sensors from MicroStrain were utilized, offering significant convenience compared to the conventional wired sensors. The use of wireless sensors allows for a rapid and flexible layout on the ferry dock without disrupting its operating schedule. A total of 16 G-Link 200 3-axis sensors with waterproof covers were deployed. These sensors transmit data to a WSDA-2000 gateway, which is capable of communicating with a computer equipped with software from the sensor provider. The sampling frequency was set to 128 Hz, and the accelerometer’s range was adjusted to the lowest possible setting of ±2 g to enhance noise density, which the supplier specifies as 25 $\mu g/\sqrt{Hz}$. The sensors are mounted directly to the steel deck using magnetic plates from the sensors. The sensor layout is shown in Fig. 2.

System Identification

Modal Analysis

Acceleration time series graphs from the field measurement are illustrated in Fig. 3. It is possible to recognize notable events when the ferry docks, such as the adjustment of the lifting towers to allow the ferry to dock and leave, or the movement from vehicles on the docking bridge. After the ferry was undocked from the docking bridge, walking excitation was performed to simulate ambient noise, a crucial input for operational modal analysis.

The acceleration recorded from walking excitation has been used to perform modal analysis. Before applying covariance driven stochastic subspace identification (SSI) algorithm to identify modal information, the data was high-passed filtered

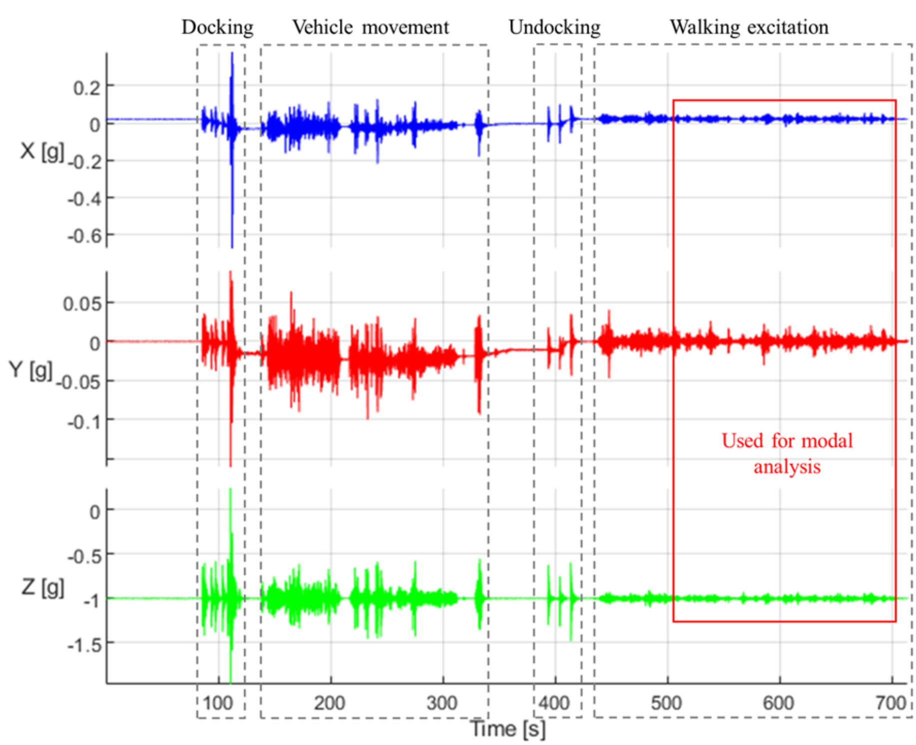

Fig. 3 Time series of accelerometer 147 during docking event of a Ferry. Direction X, Y and Z refer to longitudinal, transverse and vertical direction of the ferry dock

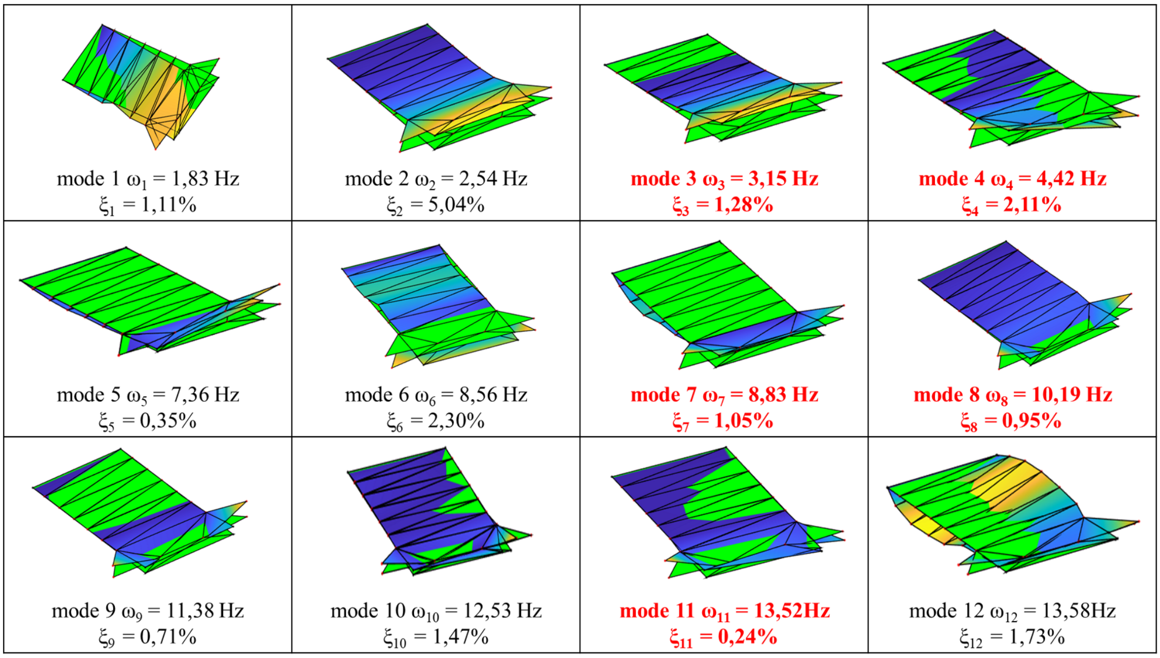

Fig. 4 Modal information from SSI: mode shapes, eigenfrequencies and damping in free state operation. Five modes noted in bold red color are chosen for the updating process

with a cut-off frequency of 0.5 Hz. The following parameters were used for SSI procedure: the number of orders was set to 200, number of blockrows was set to 100 and the number of blocks for covariance of the subspace matrix was set to 20. Finally, the mode shapes and natural frequencies are summarized in Fig. 4.

Figure 4 shows that, aside from the translation mode (mode 1), both bending and torsion modes have been identified. Modes 2, 3, 5, 6, and 7 correspond to the first and second bending modes of the entire bridge, while modes 8 to 11 indicate bending in the transverse direction of the bridge's tip. Torsional behavior is observed in modes 4 and 12. In some cases, two modes exhibit similar mode shapes, making it difficult to distinguish between them. The reason for this is believed to be the stiffness of the lifting towers. Since these towers lift the bridge using jacks, their stiffness is not stable, leading to similar mode shapes with different natural frequencies. It is important to note that modes 5, 10, and 12 exhibit unsymmetrical behavior. Given that the main structural elements are symmetric, this unsymmetrical behavior could indicate a change in the bridge's stiffness on one side over time. Five modes noted in bold red color in Fig. 4 are chosen for the updating process.

Finite Element Model Updating

Finite Element Model

An Finite element (FE) model, shown in Fig. 5, was constructed using ABAQUS [11] based on the existing drawings provided by the municipality [12]. However, some information regarding the side balconies was missing and therefore thicknesses were based on field measurements. The following cross sections were assigned to the main structural components: main beam: HE550B; cross beam: IPE240, HE240A, and UNP220; lifting beam: HE450B; diagonal bracing (L-shape): 200x200x16; and various plates with thicknesses ranging from 10 mm to 45 mm. These parts are constructed from St52-3N or RSt-37-2 steel, which have mechanical properties equivalent to the S235 and S275 steel types, respectively. Quadrilateral finite membrane-strain shell elements with reduced integration (S4R) were selected for the FE model. A mesh size sensitivity analysis for the ferry quay was conducted in [13], revealing that a mesh size between 50 mm and 100 mm is optimal. In this study, a mesh size of 50 mm was selected.

Only the structural components were modeled in ABAQUS. To accurately simulate the total mass of the docking bridge, non-structural mass was introduced to account for elements such as railings and steel gratings. The weight information for these parts was obtained from the existing drawings. The steel gratings were modeled at 90 kg/m², the large railings at approximately 81 kg/m, and the small railings at 19.25 kg/m. Ultimately, the entire structure weighed 53.64 tons.

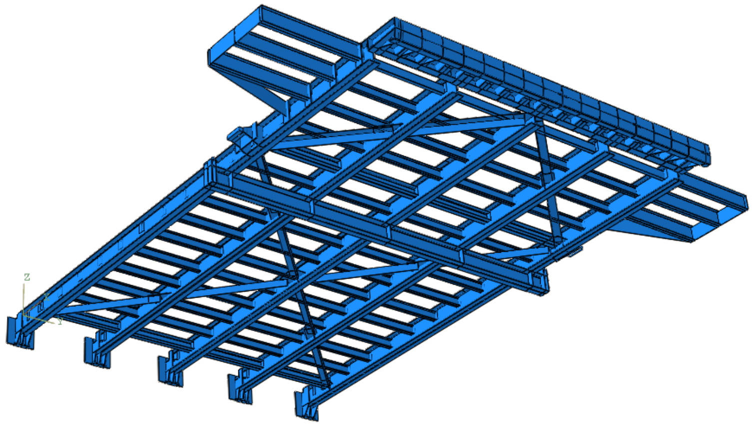

Fig. 5 Finite element model of Magerholm ferry dock in ABAQUS

As described in section 2.1, the docking bridge is supported by the abutment and lifting towers in its free state. Consequently, constraints in the transverse and vertical directions are introduced at the abutment. Springs with a stiffness of 2000 kN/m (as specified by the provider) are modeled in the longitudinal direction at the positions of the conical fenders. The lifting towers, which support the bridge vertically, are represented by vertical springs. The initial stiffness of these springs was set at 10 000 kN/m, as the exact value is unknown and will be updated later. The mode shapes extracted from FE model are depicted in Fig. 6.

Model Updating Methodology

In this study, Mottershead's sensitivity method [14] is applied to update the finite element model. This process is similar to an optimization problem, where the goal is to minimize the error between the FE model's output and the field measurement results, thereby improving the approximation of the computer model to the actual state of the structure. The output used for comparison in this study is the natural frequency of the linkspan. To align the model output as closely as possible with the measured data, the input parameters θ of the FE model—such as material density, Young's modulus, cross-sectional

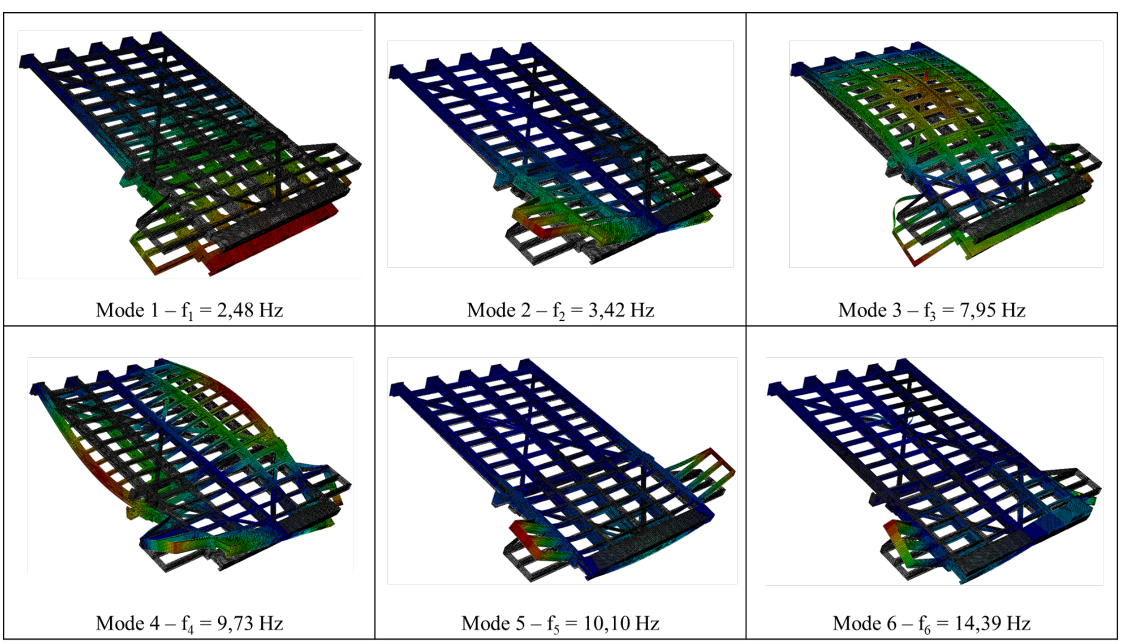

Fig. 6 First six modes of FE model

properties, etc—are systematically adjusted. This adjustment is represented by $\Delta\theta$, where $\Delta\theta_i = \theta - \theta_i$. These parameters are iteratively modified, until this quantity gradually approaches an acceptable small value:

$$J(\Delta\theta) = \epsilon_z^T W \epsilon_z \tag{1}$$

Here, W is a weighting matrix that accounts for the importance of different terms in the vector ϵ_z. It is defined as a diagonal matrix with diagonal values equal to $1/f_i^2$, where f_i are the measured frequencies in Hertz (Hz). The vector ϵ_z represents the difference between the FE model-calculated results $z(\theta)$ and the measured results z_m:

$$\epsilon_z = z_m - z(\theta) \tag{2}$$

In the iterative process, this difference can be expressed as $r_i = z_m - z(\theta_i)$. To minimize the error in each iteration, ϵ_z is updated by linearizing the non-linear relationship between θ and $z(\theta)$ as follows:

$$\epsilon_z \approx r_i - G_i \Delta\theta_i \tag{3}$$

G_i is the sensitivity matrix computed by

$$G_i = \left[\frac{\partial z_j}{\partial \theta_k}\right]_{\theta=\theta_i} \tag{4}$$

To avoid matrix singularity and ill-conditioning problem, it should be noted that all mentioned vectors and matrices should be normalized as presented in [15]. Replacing ϵ_z in Eq. (1) by (3) one can define the objective function:

$$J(\Delta\theta_i) = \| -W^{1/2} G_i \Delta\theta_i + W_i^{1/2} r_i \| \tag{5}$$

When Eq. (5) is applied in this study, with natural frequency as the quantity of interest, it is transformed as follows:

$$J(\Delta\theta_i)^* = \sum_{j=1}^{5} [W]_{j,j} \left(\frac{f_{m,j} - f_{n,j}}{f_{0,j}}\right)^2 \tag{6}$$

Here $f_{m,j}$ and $f_{n,j}$ are the j^{th} measured and numerical frequencies respectively while $f_{0,j}$ is the j^{th} initial numerical frequencies.

This optimization problem is solved using the *scipy.optimize.lsqn* function in Python. During each iteration, the parameters are updated by an amount $\Delta\theta$, which is the solution from the previous iteration:

$$\theta_{i+1} = \theta_i + \Delta\theta_i \tag{7}$$

The iteration process continues until the error between the FE model and the measurement results is reduced to an acceptable level, or when the values of θ_{i+1} and θ_i converge and are sufficiently close to each other. The workings of this algorithm have been previously presented by [15], where they also provide a code implementation of this method [16].

In practice, the FE model and measurement results yield various natural frequencies and mode shapes. Selecting which natural frequencies and mode shapes from the FE model to compare with the measured data is a challenge that needs to be addressed. To tackle this, a Mode Matching Index (MMI) has been introduced to find the natural frequencies and mode shapes of the FE model that closely match those of the measurement results. This is done based on the natural frequency values and the similarity in mode shapes, as quantified by the Modal Assurance Criterion (MAC) value

$$MMI = (1-\gamma) MAC_{m,n} - \gamma \frac{|f_m - f_n|}{f_m} \tag{8}$$

where f_m and f_n are measured and numerical frequencies respectively. To weight between mode shapes and frequencies, coefficient γ is introduced and has the range between 0 and 1. The value of γ is chosen as 0.5 in this study. For the updating purpose, only FE modes that have MAC value above 0.6 compare to measure modes, are selected for updating process.

Updating Parameters

It is important that the number of natural frequencies used for updating needs to be larger than the number of parameters to ensure unique solutions to the optimization problem [15]. The number of parameters also depends on the availability of the measured modes. In this study, four parameters were chosen; therefore, at least five natural frequencies must be used for

Table 1 Used parameters for updating routine and their limits

Paremeter	Initial value	Allowable change between iterations	Global bounds
ρ_{steel}	7850 kg/m^3	$\pm 5\%$	no bounds
k_1	10000 kN/m	$\pm 20\%$	no bounds
k_2	10000 kN/m	$\pm 20\%$	no bounds
E_{steel}	210 GPa	$\pm 5\%$	no bounds

finite element model updating. The first parameter chosen is the material density, ρ_{steel}, which accounts for possible errors in estimating non-structural mass and modeling errors. This is followed by Young's Modulus, E_{steel}, that can be associated with uncertainties in structural stiffness due to corrosion and degradation. The stiffness of the lifting towers, k_1 and k_2, is also included, as the support characteristics of this type are unknown. The parameters and their ranges are summarized in Table 1. Based on the study conducted in [13], the initial values for the stiffness of lifting towers were set to be 10000 kN/m. Allowable change of 5% was applied for steel density and Young's modulus since these two parameters were not expected to change much. However, considering the potential variability in lifting tower stiffness, a more substantial allowable change of 20% was established.

Results

The FEMU process was conducted for six iterations to minimize the objective function $J(\Delta\theta_i)^*$, as detailed in Fig. 8. A significant reduction in this quantity occurred within the first three iterations, followed by a gradual convergence. Updated parameter values are presented in Table 2, while the FEMU process's effectiveness in matching natural frequencies and mode shapes between the measured state and FE model is summarized in Table 3.

As anticipated, the stiffnesses of the lifting towers underwent the most substantial changes. Given that all measured frequencies exceeded those of the initial FE model, indicating a stiffer-than-estimated actual ferry dock state, the FEMU process increased values of the stiffness of the lifting towers. This is also reflected by a slight increase in Young's modulus. Conversely, a minor decrease in steel density might be attributed to modeling errors at joints and an inaccurate estimation of the side balconies' weight.

Figure 7 presents sensitivity index values (calculated using Eq. (4)) for the four considered parameters. The sensitivity indices of the lifting tower stiffnesses, G_{k1} and G_{k2}, reveal their primary influence on the natural frequencies of the first bending and first torsional modes. Their impact on other modes is less pronounced.

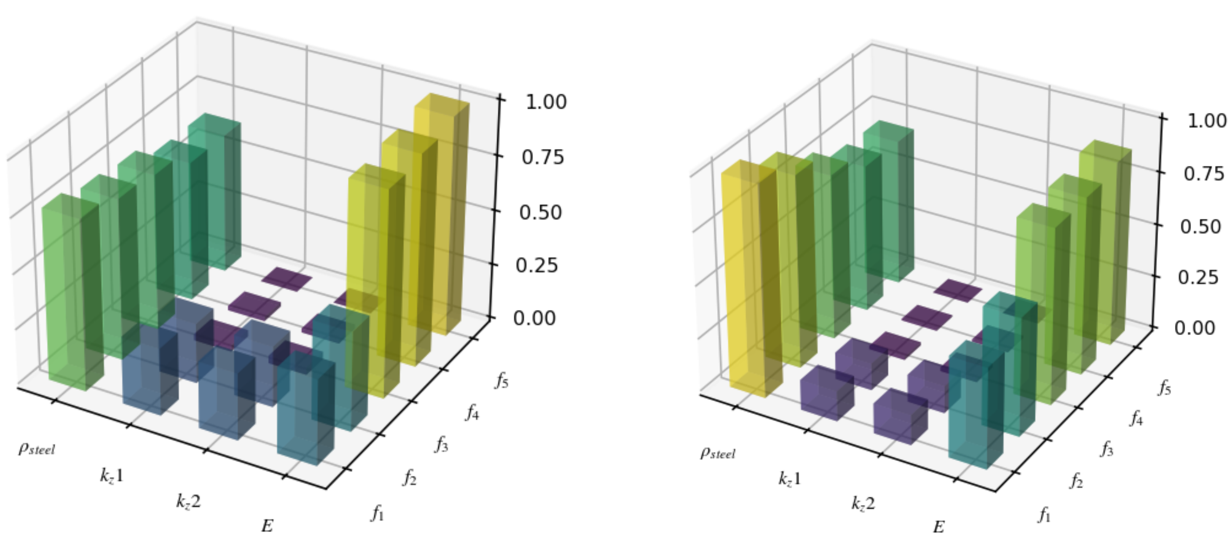

(a) Scaled sensitivity matrix of first iteration

(b) Scaled sensitivity matrix of last iteration

Fig. 7 Scaled sensitivity matrix of FEMU process

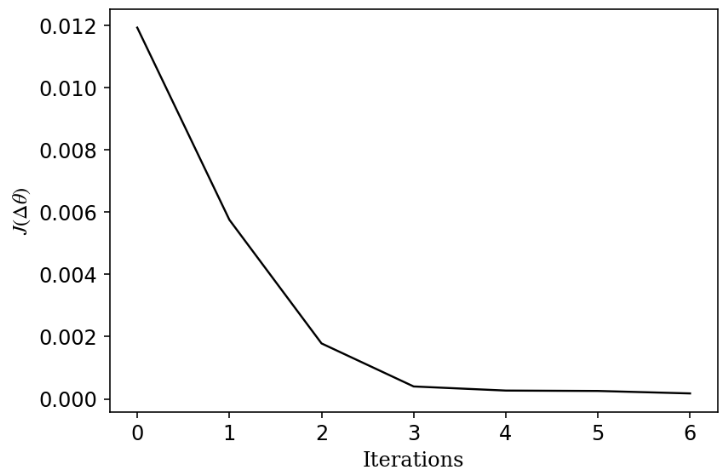

Fig. 8 Objective function $J(\Delta\theta_i)^*$ through iterations

Table 2 Parameter values before and after finite element updating

Paremeter	Initial value	Updated value	Change
ρ_{steel}	7850 kg/m^3	7039 kg/m^3	-811 kg/m^3
k_1	10000 kN/m	20736 kN/m	10736 kN/m
k_2	10000 kN/m	20736 kN/m	10736 kN/m
E_{steel}	210 GPa	218.9 GPa	8.9 GPa

Table 3 Natural frequencies and MAC values before and after updating

Mode	Frequency, f[Hz]							MAC value		
	Measured	Initial	Error[%]	Weighted errors[%]	Updated	Error[%]	Weighted errors[%]	Initial	Updated	Change
1	3.15	2.48	-21.27	-11.92	3.18	0.95	0.53	0.957	0.981	0.024
2	4.42	3.42	-22.62	-6.44	4.26	-3.62	-1.03	0.953	0.977	0.024
3	8.83	7.95	-9.97	-0.71	8.63	-2.27	-0.16	0.649	0.664	0.015
4	10.19	10.1	-0.88	-0.05	10.84	6.38	0.34	0.960	0.958	-0.002
5	13.52	14.39	6.43	0.20	15.2	12.43	0.38	0.699	0.703	0.004
Absolute average			**10.2**			**4.3**		**0.70**	**0.71**	

The updating process yielded a commendable reduction in average frequency errors from 10.2% to 4.3%. Notably, the most significant improvements were observed for the first two modes, aligning with the amplified weighting assigned to these modes. A slight increase in the MAC value suggests a closer approximation of the FE model's mode shapes to those extracted from measurements.

Sensitivity Analysis of Lifting Towers

One of the motivations for performing studies at Magerholm as a case study stems from the collapse of its ferry dock during Ingunn storm, one of the most powerful storms to impact Norway in 30 years [17], on 31^{st} January 2024. Following the storm, the entire deck of the structure detached from the lifting towers and sank into the water, necessitating a salvage operation and reattachment to the towers. Although the exact cause of the collapse remains uncertain, the authors suspect that similar damages can be caused by failure of the lifting towers. Consequently, the authors conducted a sensitivity analysis on the updated model of lifting tower stiffness to assess its impact on the dynamic behavior of the linkspan.

The results are presented in Figs. 9 and 10. Figure 9 captures the sensitivity of frequencies when changing the stiffness of one tower and keep the other one constant at $k = 20736 kN/m$ which is the stiffness of the towers after updating. On the other hand Fig. 10 capture that when changing the stiffness of both towers at the same time.

As expected, there is a clear correlation between tower stiffness and modal behavior. Most modes are sensitive to stiffness variations, except for mode 6, which remains relatively unaffected. The first bending mode (mode 1) is particularly sensitive to stiffness changes, while modes 3 and 6 show minimal sensitivity. Interestingly, the first torsional mode (mode 2) exhibits

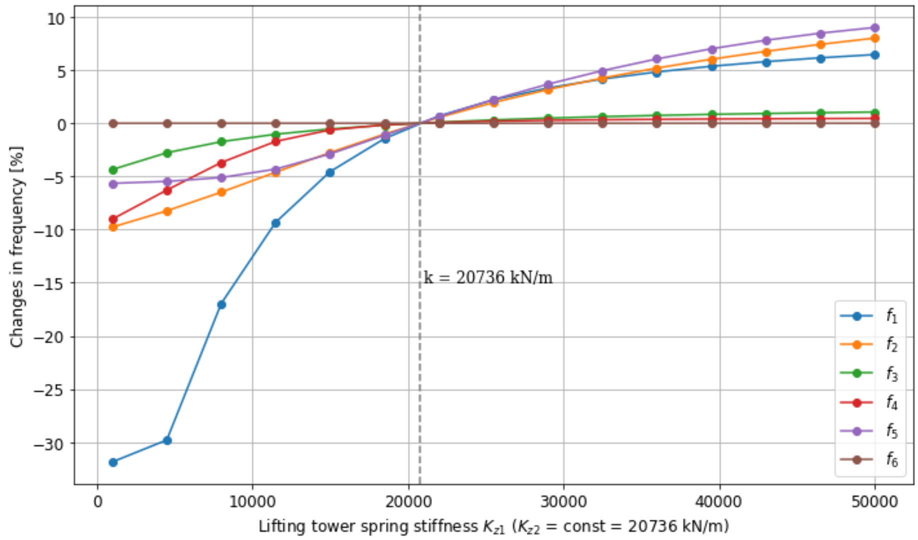

Fig. 9 Percentage changes in natural frequencies of 6 modes corresponded to different lifting tower stiffness values - Altering stiffness in a single tower. $k = 20736kN/m$ is the stiffness of the towers after updating process

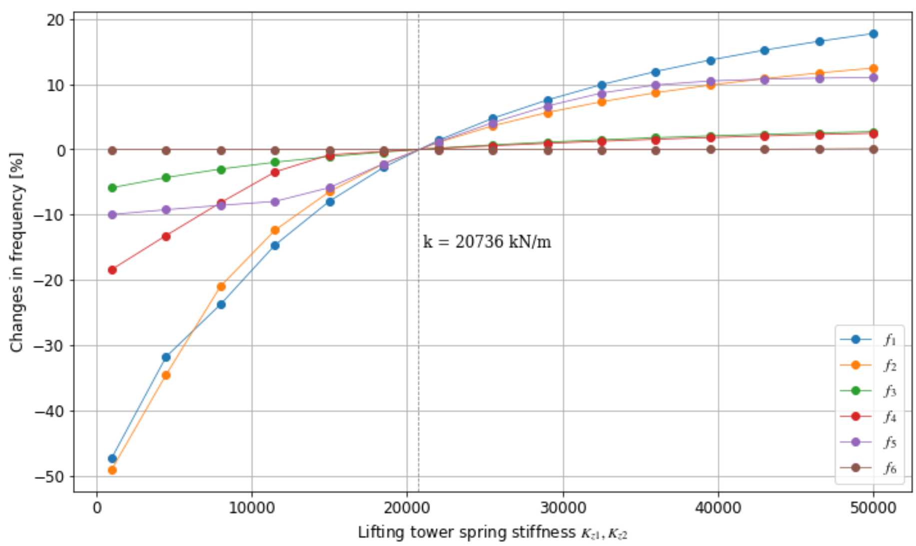

Fig. 10 Percentage changes changes in natural frequencies of 6 modes corresponded to different lifting tower stiffness values - Altering stiffness in both towers. $k = 20736kN/m$ is the stiffness of the towers after updating process

significantly increased sensitivity when both tower stiffnesses are adjusted. Other modes experience a gradual frequency increase with rising stiffness.

Conclusion

This study provides a better understanding of the modal behavior of linkspans and examines the possibility of detecting lifting tower damage modeled by reduction in its stiffness using modal information. The key points can be summarized as follows:

- When employing wireless accelerometers, walking excitation serves as an effective input for the SSI algorithm in determining the modal characteristics of linkspans.

- There are challenges in selecting modes for FEMU application due to multiple modes with similar mode shapes and closely spaced natural frequencies. This is caused by the variable stiffness of the jacks used in lifting towers, which can fluctuate slightly during operation, resulting in nearly identical modes.
- Sensitivity-based FEMU has proven highly effective in constructing a FE model that replicates the actual condition of the linkspan. The error between the FE model and field measurement results was reduced to less than 5% within just six updating iterations.
- The sensitivity analysis shows a strong correlation between lifting tower stiffness and the docking bridge natural frequencies, especially when the stiffness of lifting towers is below 20,000 kN/m.
- While most modes are sensitive to stiffness variations, the first bending and first torsional modes are particularly susceptible to changes in lifting tower stiffness. This suggests that damage to the lifting towers would likely be reflected in changes to the natural frequencies of these two modes. After the updating process, the stiffness of lifting towers is estimated to be approximately 20,000 kN/m.

Acknowledgments The study was conducted with support from the Research Council of Norway through the Norwegian Regional Research Fund in Møre og Romsdal county (SHMBru project 331578). The authors gratefully acknowledge Møre og Romsdal fylke for financing the research and for helping during the planning and execution of instrumentation and measurements.

References

1. U. S. Department of Homeland Security Science and Technology. "Aging Infrastructure: Issues, Research, and Technology" (2010).
2. Kim, K.H., Nam, M.S., Hwang, H.H., and Ann, K.Y. "Prediction of remaining life for bridge decks considering deterioration factors and propose of prioritization process for bridge deck maintenance". *Sustain*, 12:1–25 (2020).
3. Noortwijk, J.M.V. and Klatter, H.E. "The use of lifetime distributions in bridge maintenance and replacement modelling". *Computers & Structures*, 82:1091–1099 (2004).
4. Jeong, Y., Kim, W.S., Lee, I., and Lee, J. "Bridge service life estimation considering inspection reliability". *KSCE Journal of Civil Engineering*, 21:1882–1893 (2017).
5. Agdas, D., Rice, J.A., Martinez, J.R., and Lasa, I.R. "Comparison of visual inspection and structural-health monitoring as bridge condition assessment methods". *Performance of Constructed Facilities*, 30(3):1–10 (2016).
6. Moughty, J.J. and Casas, J.R. "A state of the art review of modal-based damage detection in bridges: Development, challenges, and solutions". *Applied Sciences*, 7 (2017).
7. Srikanth, I. and Arockiasamy, M. "Deterioration models for prediction of remaining use-ful life of timber and concrete bridges: A review". *Traffic and Transportation Engineering*, 7:152–173 (2020).
8. Vegvesen, S. *Hånbok – Ferjestatistikk*. V620 (2018).
9. Siedziako, B. and Nord, T.S. *Experimental vibration analysis on the Rykkjem ferry dock during ferry berthing*. Presented on IMAC-XLI (In press) (2023).
10. Vegvesen, S. "Ferjestatistikk" (2024). Last accessed 20 August 2024.
11. Dassault Systemes Simulia Corp. "Abaqus/CAE 6.14 – Documentation" (2014).
12. Statens Vegvesen 2022 Brutus. "Management system for bridges, ferry quays and other load- bearing structures in Norway" (2022).
13. Siedziako, B., Nord, T.S., and Fenerci, A. "Finite element model updating of a ferry dock bridge". *Journal of Physics: Conference Series*, 2647:182001 (2024).
14. Mottershead, J.E., Link, M., and Friswell, M.I. "The sensitivity method in finite element model updating: A tutorial". *Mechanical Systems and Signal Processing*, 25:2275–2296 (2011).
15. Bjørn T. Svendsen, G.T.F., Øyvind W. Petersen and Rønnquist, A. "Improved finite element model updating of a full-scale steel bridge using sensitivity analysis". *Structure and Infrastructure Engineering*, 19(3):315–331 (2023).
16. Bjørn T. Svendsen, G.T.F., Øyvind W. Petersen and Rønnquist, A. "Fe model updating in python" (2020).
17. "New wind record in norway with storm ingunn". https://www.meteoiq.com/2024/02/02/new-wind-record-in-norway-with-storm-ingunn/Posted on 2.02.2024 by Dennis Schulze.